Quantum tunneling decay due to interference of a bound and an antibound state

Gastón García-Calderón [*]
Instituto de Física, Universidad Nacional Autónoma de México, Apartado Postal 20 364, 01000 Mexico City, Mexico

Roberto Romo [†]
Facultad de Ciencias, Universidad Autónoma de Baja California, Apartado Postal 1880, 22800 Ensenada, Baja California, Mexico

(Received 29 December 2023; accepted 8 May 2024; published 23 May 2024)

We consider an exact analytical formulation of the wave function for quantum tunneling decay, given as an expansion in terms of the bound, antibound, and resonant states, for the time-honored problem of a particle initially confined by a potential. We find that the interference term between a bound state and its corresponding antibound state may favor a decay process in which the probability density spreads throughout space in a nonexponential fashion.

DOI: 10.1103/PhysRevA.109.052225

I. INTRODUCTION

Quantum tunneling decay corresponds to the time evolution of a particle initially confined by a potential barrier that decays to the outside by tunneling. Work on quantum tunneling decay has usually been focused on the description of the exponential decaying regime and its deviation at very short or very long times with respect to the lifetime of the system [1–8].

In this paper we make use of a rigorous non-Hermitian approach based on the analytical properties of the outgoing Green's function, which so far has been used extensively to study the decaying regimes mentioned above [9–12], to investigate the effect of bound and antibound states on tunneling decay. Contrary to the widespread view that these states do not contribute to the decay process, we show that the interference between a bound state and its corresponding antibound state may exhibit a decaying regime that is purely nonexponential. It may be of interest to mention that a purely nonexponential decay behavior has been reported before for a decaying system subjected to a constant electric field [13]; however, in that case there were no bound or antibound states. The result presented here involves exact numerical calculations of the behavior with time of the nonescape probability, which refers to the integrated probability density along the internal region of the potential and of the probability density along the external interaction region.

It may be worth recalling that the usual Hermitian approach involving the energy continuum may also be obtained from the analytical properties of the outgoing Green's function to the problem [14]. It may be shown that the Hermitian and non-Hermitian approaches lead to the same numerical results for quantum tunneling decay of resonant and continuum states [9,15]. The Hermitian approach, however, rests on a "black-box" type of numerical calculation, and hence, in order to attain physical insight on the decay process it usually relies on analytical approximations that limit the general validity of its results and also do not favor the search for novel phenomena.

II. FORMALISM

For the sake of completeness of the discussion and to fix the notation we briefly discuss some features of the non-Hermitian formalism of quantum tunneling decay. Let us consider the decay of a state $\Psi(x,0)$, initially confined, at $t=0$, along the internal region $0 \leqslant x \leqslant L$ of a potential $V(x)$ on the half-line $\in (0,\infty)$, which vanishes exactly beyond a certain distance, i.e., $V(x)=0$ for $x \geqslant L$. As is well known, the solution $\Psi(x,t)$ as time evolves may be expressed in terms of the retarded Green's function $g(x,x';t)$ of the problem as

$$\Psi(x,t) = \int_0^L g(x,x';t)\Psi(x',0)\,dx'. \tag{1}$$

One may solve Eq. (1) by Laplace transforming $g(x,x';t)$ into the wave number k plane to make use of the analytical properties of the outgoing Green's function $G^+(x,x';k)$ of the problem. This allows us to write $G^+(x,x';k)$ as an expansion involving the full set of poles $\{\kappa_n\}$ of the problem, which includes those belonging to the bound, antibound, and resonant states of the system, as described in Refs. [7,15],

$$G^+(x,x';k) = \left(\frac{2m}{\hbar^2}\right)\left(\frac{1}{2k}\right)\sum_n \frac{u_n(x)u_n(x')}{k-\kappa_n}, \tag{2}$$

which holds for $(x,x') < L$ and also for $x < L$ and $x' = L$ and vice versa [7]. The functions $\{u_n(x)\}$ in (2) follow from the residues of $G^+(x,x';k)$ at their poles, which also provides the normalization condition for these states [7,16],

$$\int_0^L u_n^2(x)\,dx + \frac{i}{2\kappa_n}u_n^2(L) = 1. \tag{3}$$

[*] gaston@fisica.unam.mx
[†] romo@uabc.edu.mx

Note that for bound states, the second term on the left in the above expression may be written as the integral of $u_n(x)$ from L to infinity, which leads to the usual normalization rule for these states.

The complex poles that follow from the above considerations are simple, except in special circumstances where double or higher-order poles may be present [14]. The poles are distributed on the complex k plane in a well-known manner [14] and are located either in the lower half of the k plane, distributed symmetrically with respect to the imaginary k axis, or on that axis corresponding to bound states for positive and antibound states for negative imaginary-pole values. The complex poles located on the third quadrant of the k plane and its corresponding residues, κ_{-r} and $u_{-r}(x)$, are related by time-reversal invariance to those on the fourth quadrant by the relations $\kappa_{-r} = -\kappa_r^*$ and $u_{-r}(x) = u_r^*(x)$ [17].

The location of the poles of the outgoing Green's function of the problem, or, equivalently in the present discussion, of the scattering function of the problem, is a function of the parameters of the potential [18]. They may be calculated using well-known iterative methods such as the Newton-Raphson method [19]. In the case of a potential initially having a vanishing well, one may see that as the well depth increases, each complex pole $\kappa_r = \alpha_r - i\beta_r$ and its symmetric counterpart $\kappa_{-r} = -\kappa_r^*$ move towards the imaginary axis, where they meet and become a double antibound pole that, as the well depth further increases, splits in two poles located on the imaginary k axis. One pole goes up to become a bound pole after crossing the origin at $k = 0$, whereas the other pole goes downwards and remains an antibound pole. Bound and antibound poles are no longer symmetric with each other.

The functions $u_n(x)$ satisfy the Schrödinger equation of the problem with the boundary condition at $x = 0$,

$$u_n(0) = 0, \tag{4}$$

and the outgoing boundary condition at $x = L$ [1,7,15],

$$u_n'(L) = i\kappa_n u_n(L), \tag{5}$$

where $u_n'(L) \equiv [(d/dx)u_n(x)]_{x=L}$. It may be worth recalling that along the external interaction region, the Schrödinger equation for real energy $E = (\hbar^2/2m)k^2$, and hence for a real wave number k, is given, in general, as a linear combination of outgoing and incoming waves, $A(k)\exp(ikx) + B(k)\exp(-ikx)$. In order to describe the decaying process, Gamow imposed the absence of incoming waves in the above solution, namely, $B(k) = 0$ [1,2]. The above condition corresponds to the poles of the outgoing Green's function of the problem.

Along the energy continuum, the complex energy eigenvalues $E_r = (\hbar^2/2m)\kappa_n^2 = \mathcal{E}_r - i\Gamma_r/2$, where the complex wave numbers $\kappa_r = \alpha_r - i\beta_r$, imply that the corresponding eigenfunctions as a function of the distance along the external interaction region behave as

$$|u_r(x)|^2 = |A_r e^{i\kappa_r x}|^2 \sim e^{2\beta_r x}, \quad x \geqslant L, \tag{6}$$

which shows that $|u_r(x)|^2$ diverges exponentially with distance. For antibound states, where, as mentioned above, $\kappa_a = -i\gamma_a$ and hence $E_a = -(\hbar^2/2m)\gamma_a^2$ is real, the corresponding eigenfunctions $u_a(x) \sim \exp(\gamma_a x)$ for $x \geqslant L$ also diverge as distance increases. As a consequence, the usual rules of normalization and eigenfunction expansions do not hold for resonant and antibound states. The action of the Hamiltonian on the eigenfunctions $u_r(x)$ and $u_a(x)$ is not on the Hermitian sector of the domain of the Hamiltonian, and hence, it determines their non-Hermitian character. As is well known, this is not the case for bound states, which correspond to positive imaginary poles $\kappa_b = i\gamma_b$, real energies $E_b = -(\hbar^2/2m)\gamma_b^2$, and eigenfunctions $u_b(x) \sim \exp(-\gamma_b x)$ that vanish at large distances, exhibiting their Hermitian character.

As pointed out above, the analysis of the tunneling decay process based on the analytical properties of the outgoing Green's function has led to a non-Hermitian formulation that solves the problems of the normalization and resonant expansions that limited the approach by Gamow. It follows, then, that the decaying wave solution [7,15] along the internal interaction region may be written as

$$\Psi(x,t) = \sum_n C_n u_n(x) M(y_n^\circ), \quad x \leqslant L, \tag{7}$$

and that along the external region may be written as

$$\Psi(x,t) = \sum_n C_n u_n(L) M(y_n), \quad x \geqslant L, \tag{8}$$

where the index n in sums (7) and (8) runs over the full set of bound states b, antibound states a, and resonant states r and $-r$ of the problem.

The coefficients C_n in the above expressions read

$$C_n = \int_0^L \Psi(x,0) u_n(x)\, dx. \tag{9}$$

The functions $M(y_n)$ in (8) are defined as [15,17]

$$\begin{aligned} M(y_n) &= \frac{i}{2\pi}\int_{-\infty}^{\infty} \frac{e^{ik(x-L)}e^{-i\hbar k^2 t/2m}}{k-\kappa_n} dk \\ &= \tfrac{1}{2} e^{im(x-L)^2/2\hbar t} w(iy_n), \end{aligned} \tag{10}$$

where the argument y_n is given by

$$y_n = e^{-i\pi/4}\left(\frac{m}{2\hbar t}\right)^{1/2}\left[(x-L) - \frac{\hbar\kappa_n}{m}t\right] \tag{11}$$

and the function $w(iy_n) = \exp(y_n^2)\mathrm{erfc}(y_n)$ stands for the Faddeyeva-Terent'ev function [20,21], for which efficient computational methods to calculate it exist [22]. The argument y_n° of the function $M(y_n^\circ)$ in (7) is that of y_n with $x = L$, namely,

$$y_n^\circ = -e^{-i\pi/4}\left(\frac{\hbar}{2m}\right)^{1/2}\kappa_n t^{1/2}. \tag{12}$$

The functions $M(y_n^\circ)$ and $M(y_n)$ defined above describe the quantum transient behavior in the tunneling decay process. We shall refer to them as transient functions.

Using (7), one may write the expansion of $\Psi(x,t)$ as

$$\begin{aligned} \Psi(x,t) = &\sum_{b=1}^{N_b} C_b u_b(x) M(y_b^\circ) + \sum_{a=1}^{N_a} C_a u_a(x) M(y_a^\circ) \\ &+ \sum_{r=1}^{\infty}[C_r u_r(x) M(y_r^\circ) + C_r^* u_r^*(x) M(y_{-r}^\circ)], \end{aligned} \tag{13}$$

where N_b and N_a stand for the numbers of bound and antibound terms of the problem and the last term refers to the resonant states of the system.

If the initial state $\Psi(x,0)$ is normalized to unity, one has

$$\int_0^L |\Psi(x,0)|^2\,dx = 1, \tag{14}$$

and hence, substituting (13) for $t=0$ into (14) and using $M(0)=1/2$ [17,21], one obtains

$$\frac{1}{2}\left[\sum_{b=1}^{N_b} C_b\bar{C}_b + \sum_{a=1}^{N_a} C_a\bar{C}_a\right] + \frac{1}{2}\sum_{r=1}^{\infty}[C_r\bar{C}_r + (C_r\bar{C}_r)^*] = 1, \tag{15}$$

where the coefficients $\bar{C}_n$, with $n=b,a,r$, are given by (9) with $\Psi(x,0)$ replaced by $\Psi^*(x,0)$. It is worth noting that since the sum of the square moduli of the coefficients C_n in the above expression does not add up to the norm of the expanded function, they cannot be interpreted as probability amplitudes. However, (15) suggests that the terms $C_n\bar{C}_n$, except those corresponding to bound states, may be interpreted as quasiprobabilities. This result also manifests the non-Hermitian character of this approach.

Note also that the analysis above is equivalent to the case of zero angular momentum (s waves) for a spherical symmetric potential that also vanishes after a certain distance and may be extended to higher angular momenta in a straightforward way.

A. Role of the expansion coefficients

An interesting situation regarding decaying artificial quantum systems is that the initial state $\Psi(x,0)$ may be prepared to overlap strongly with a chosen resonant state of the system, say, $u_s(x)$. As a result, the contribution of the rest of the expansion coefficients is very small, and hence, using (15), we obtain

$$\tfrac{1}{2}[C_s\bar{C}_s + (C_s\bar{C}_s)^*] \approx 1. \tag{16}$$

Equation (16) has been used amply for potentials with zero well depth, and hence with no bound or antibound poles, providing calculations that are indistinguishable from those involving many pole terms [11,15,23], as considered for double-barrier resonant tunneling structures [24,25] and ultracold gases [23,26].

Without loss of generality, we may initially consider a barrier potential with a well of vanishing depth and hence with no bound or antibound poles and choose the initial sate to overlap strongly with the lowest-energy resonant states having complex poles κ_1 and $\kappa_{-1}=-\kappa_1^*$ of the system, so that (16) remains valid with $s=1$. We may follow the procedure described previously, which numerically is the best suited for this purpose, of increasing the potential depth by small steps so that the complex poles with $s=1$ become the first bound and antibound poles of the system, $\kappa_b=i\gamma_b$ and $\kappa_a=-i\gamma_a$, which, as pointed out above, are no longer symmetric with each other, and hence, $\gamma_b\neq\gamma_a$. Since the shape of the corresponding eigenfunctions remains essentially unaffected by the above procedure, (16) becomes, for the bound and antibound states, the following expression:

$$\tfrac{1}{2}C_b\bar{C}_b + \tfrac{1}{2}C_a\bar{C}_a \approx 1. \tag{17}$$

According to the above considerations, the corresponding decaying wave function may then be written as

$$\Psi(x,t) \approx C_b u_b(x) M(y_b^\circ) + C_a u_a(x) M(y_a^\circ), \tag{18}$$

which holds in the whole time span except at ultrashort times when the full expansion is required [10].

In what follows we investigate the implication of Eqs. (17) and (18) for the decaying process.

III. CONTINUITY EQUATION AND PROBABILITY CURRENT DENSITY

As is well known, integration of the continuity equation along the internal interaction region may be written as

$$\frac{d}{dt}P(t) = -J(L,t), \tag{19}$$

where $P(t)$ is given by

$$P(t) = \int_0^L |\Psi(x,t)|^2\,dx, \tag{20}$$

which represents the probability, also known as the nonescape probability, to find the decaying particle at time t within the internal interaction region, and $J(L,t)$ stands for the probability current density,

$$J(L,t) = \left(\frac{\hbar}{m}\right)\mathrm{Im}\left[\Psi^*(x,t)\frac{\partial}{\partial x}\Psi(x,t)\right]_{x=L}. \tag{21}$$

The quantity $J(L,t)$ is of interest because, as follows from (19), it is proportional to the variation with respect to time of the integrated probability density along the internal interaction region, and hence, if it differs from zero, it implies a process of tunneling decay.

It is convenient to write (18) as

$$\Psi(x,t) \approx \Psi_b(x,t) + \Psi_a(x,t), \tag{22}$$

with

$$\Psi_b(x,t) = C_b u_b(x) M(y_b^\circ) \tag{23}$$

and

$$\Psi_a(x,t) = C_a u_a(x) M(y_a^\circ). \tag{24}$$

One may see that substituting (22) into (21) involves purely bound, purely antibound, and cross bound and antibound contributions that follow from (23) and (24). The resulting expression may be written as

$$J(L,t) \approx J_{bb}(L,t) + J_{aa}(L,t) + J_{ba}(L,t) + J_{ab}(L,t). \tag{25}$$

For a bound state one may calculate $J_{bb}(L,t)$ using (23) and the corresponding boundary condition for the bound-state eigenfunction $u_b(x)$, given by (5) with $\kappa_b=i\gamma_b$, to obtain, as is well known,

$$J_{bb}(L,t) = 0. \tag{26}$$

In a similar fashion, for an antibound state $u_a(x)$, where $\kappa_a = -i\gamma_a$, one may use (24) to obtain

$$J_{aa}(L,t) = 0. \tag{27}$$

The situation, however, is different for the cross terms $J_{ba}(L,t)$ and $J_{ab}(L,t)$. Let us denote by $J_{\rm ct}(L,t)$, where ct stands for cross terms, the sum of the above two terms. Then using (23) and (24) gives

$$J_{\rm ct}(L,t) = \left(\frac{\hbar}{m}\right)\mathrm{Im}[C_b C_a^* u_b(L) u_a^*(L) M(y_b^\circ) M^*(y_a^\circ)](\gamma_a - \gamma_b). \tag{28}$$

Since, in general, $\gamma_a \neq \gamma_b$, Eq. (28) shows the existence of a net probability density current coming out of the system due to the interference effect between the bound and antibound states of the system. In view of (18), one may see that the expression of $J_{\rm ct}$ given by (28) provides a flux coming out of the potential interaction.

Equation (28) represents the main result of this work. It is worth emphasizing, as shown by (26) and (27), that the flux due solely to the bound or antibound state vanishes exactly.

In previous work, using resonant states to investigate the time evolution of decay, we studied the nonescape probability and the probability density along the external region [9,11,12,15]. Here, in addition to provide the grounds to make a comparison with those studies, we also consider the effect on the decay process due to the bound, antibound, and interference contributions. For that reason we address these quantities in what follows and also in the model calculations.

IV. NONESCAPE PROBABILITY

As mentioned above, the probability that the decaying particle remains within the internal region of the potential as time evolves is given by (20). Using (18), one may write the nonescape probability $P(t)$ for the bound and antibound states as

$$P(t) = P_b(t) + P_a(t) + P_{ba}(t), \tag{29}$$

where $P_b(t)$, $P_a(t)$, and $P_{ab}(t)$ are exact analytical expressions that stand, respectively, for the bound, antibound, and corresponding interference terms, which read

$$P_b(t) = |C_b|^2 \mathcal{Y}_{bb} |M(y_b^\circ)|^2, \tag{30}$$

$$P_a(t) = |C_a|^2 \mathcal{Y}_{aa} |M(y_a^\circ)|^2, \tag{31}$$

and

$$P_{ba}(t) = 2\mathrm{Re}\{C_b C_a^* \mathcal{Y}_{ba} M(y_b^\circ) M^*(y_a^\circ)\}, \tag{32}$$

where

$$\mathcal{Y}_{ij} = \int_0^L u_i^*(x) u_j(x)\, dx \tag{33}$$

and ij stands for the distinct combinations of a or b shown in (30)–(32). The transient behavior of the above quantities is analyzed in Appendix A.

V. PROBABILITY DENSITY ALONG THE EXTERNAL REGION

Equation (17) allows us to write the decaying solution $\Psi(x,t)$ along the external interaction region $x > L$ as

$$\Psi(x,t) \approx C_b u_b(L) M(y_b) + C_a u_a(L) M(y_a), \tag{34}$$

which leads to the expression for the probability density $|\Psi(x,t)|^2$,

$$|\Psi(x,t)|^2 = |\Psi_b(x,t)|^2 + |\Psi_a(x,t)|^2 + I_{ba}(x,t), \tag{35}$$

where

$$|\Psi_b(x,t)|^2 = |C_b|^2 |u_b(L)|^2 |M(y_b)|^2, \tag{36}$$

$$|\Psi_a(x,t)|^2 = |C_a|^2 |u_a(L)|^2 |M(y_a)|^2, \tag{37}$$

and

$$I_{ba}(x,t) = 2\mathrm{Re}\{C_b C_a^* u_b(L) u_a^*(L) M(y_b) M^*(y_a)\}. \tag{38}$$

The transient behavior corresponding to the above expressions is analyzed in Appendix B.

VI. COMMENT ON THE STANDARD EXPANSION FOR THE DECAYING WAVE FUNCTION

As is well known, in the Hermitian standard formulation of quantum mechanics, the decaying wave function in k space involves a sum over bound states plus an integral over the continuum states of the problem. For the case discussed in this work the decaying wave function reads

$$\Psi(x,t) = \sum_{b=1}^{N_b} C_b u_b(x) e^{-i\hbar k_b^2 t/2m} + \int_0^\infty C(k) \psi^+(k,x) e^{-i\hbar k^2 t/2m}\, dk, \tag{39}$$

where $C(k)$ corresponds to the overlap of the initial state $\Psi(x,0)$ with the continuum wave functions $\psi^+(k,x)$,

$$C(k) = \int_0^L \Psi(x,0) \psi^{+*}(k,x)\, dx. \tag{40}$$

Conservation of the probability implies

$$\sum_{b=1}^{N_b} |C_b|^2 + \int_0^\infty |C(k)|^2 dk = 1. \tag{41}$$

It is of interest to compare (15) and (41). Both expressions are analytically exact but exhibit distinct features of the non-Hermitian and Hermitian formulations. They have the same notion for bound states, except that in the former there is a factor of (1/2). The above expressions also differ in regard to the notions of antibound and resonant states for the non-Hermitian case and that of continuum states for the Hermitian one. The relationship between the continuum and resonant states is well understood through the notion of resonance [27]. That is not the case for antibound states, which presumably must arise from an interference process involving the bound and continuum states. This requires further elucidation. Another important issue is the nature of the quasiprobabilities corresponding to (15), as mentioned at the end of Sec. II.

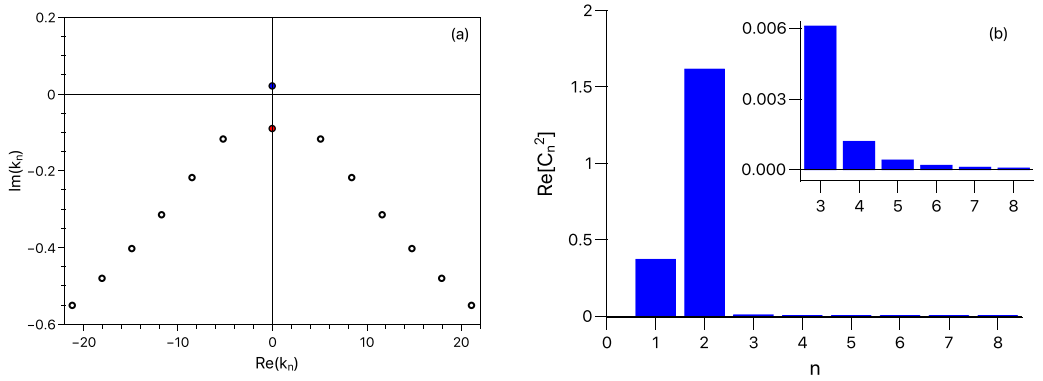

FIG. 1. (a) exhibits the location on the k plane of the bound, antibound, and a few complex poles for the Picasso model with parameters discussed in the text. (b) displays the values of the real part of the expansion coefficients $\mathrm{Re}[C_n^2]$ for several pole terms n. Here $n = 1$ and $n = 2$ refer, respectively, to the bound and antibound contributions, and the inset shows the very small values of the remaining expansion coefficients. See text.

VII. MODEL CALCULATIONS

In order to illustrate the results obtained in this work we consider the Picasso model [28], which consists of a finite rectangular potential $V(x)$ of depth $-U_0$ with radius $x = L$ and a δ potential of intensity $\lambda > 0$ located at the boundary value $x = L$, that is,

$$V(x) = -U_0\Theta(L - x) + \lambda\delta(x - L). \tag{42}$$

Here for the simplicity of the description in the following we choose natural units $\hbar = 2m = 1$. As discussed previously, the potential parameters determine the location of the poles $\{\kappa_n\}$ on the k plane and the corresponding eigenfunctions $\{u_n(x)\}$. Another relevant input for the calculations is the initial state. Previous work supports the view that except at ultrashort times [10], the specific analytical expression for the initial state is not essential to determine the decaying behavior of the system, but the values of the expansion coefficients of the decaying wave function [25]. Hence, for the simplicity of the discussion we choose as the initial state the infinite-wall-box model state,

$$\Psi(x, 0) = \sqrt{\frac{2}{L}}\,\sin\left(\frac{\pi}{L}x\right). \tag{43}$$

Figure 1(a) exhibits the bound pole κ_b, the antibound pole κ_a, and the first six complex poles κ_r with the symmetric counterparts κ_{-r} corresponding to the parameters $\lambda = 15.0$, $U_0 = -8.69$, and $L = 1.0$. The bound and antibound poles are located at $\kappa_b = 0.0208\,i$ and $\kappa_a = -0.0910\,i$. Figure 1(b) provides a plot of the expansion coefficients $\mathrm{Re}\,[C_n^2]$ vs n. Notice that the contribution of the resonant coefficients $n =$ 3–8 is much smaller than the bound and antibound contributions given by $\mathrm{Re}[C_b^2] = 0.3693$ and $\mathrm{Re}[C_a^2] = 1.6147$, respectively. In fact, Eq. (17) yields a value of 0.992, which implies that most of the strength is shared by the bound and antibound contributions.

Figure 2 shows a plot of the nonescape probability $P(t)$ (blue line) vs the time t and the corresponding bound $[P_b(t)]$, antibound $[P_a(t)]$, and interference $[P_{ba}(t)]$ contributions given by (29)–(32), as indicated in the legend. Note the initial transient drop of $P(t)$ at short times, which indicates the existence of tunneling decay, followed by an essentially constant behavior that implies the end of the tunneling process. Note also that the oscillatory behavior of $P_b(t)$ (red dashed line) is canceled out by that of $P_{ba}(t)$ (orange dot-dashed line) and that the antibound contribution (black dotted line) essentially vanishes after the initial drop in $P(t)$.

Each of the three panels in Fig. 3 provides a plot of the dynamical behavior of the probability density $|\Psi(x, t_0)|^2$ along the external interaction region as a function of distance x/L at fixed times t_0, as indicated in each panel. Each panel differs by a factor of 10, both for the value of t_0 and for the distance x/L. A comparison of the panels shows that the bump structure propagates. Note, however, from the analysis of the arguments of the terms $M(y_b)$ and $M(y_a)$ discussed above, that there is no distinguishable propagating wave front like what occurs in the tunneling decay involving a sharp resonant state [11]; instead, it spreads in a nonexponential fashion. To the left and right of the maximum height of the bump structure in each panel, the distances $x_b = 2\gamma_b t_0$ and $x_a = 2\gamma_a t_0$ (in units of L), indicated respectively by triangles, suggest that γ_b and γ_a may be visualized as some type of velocities.

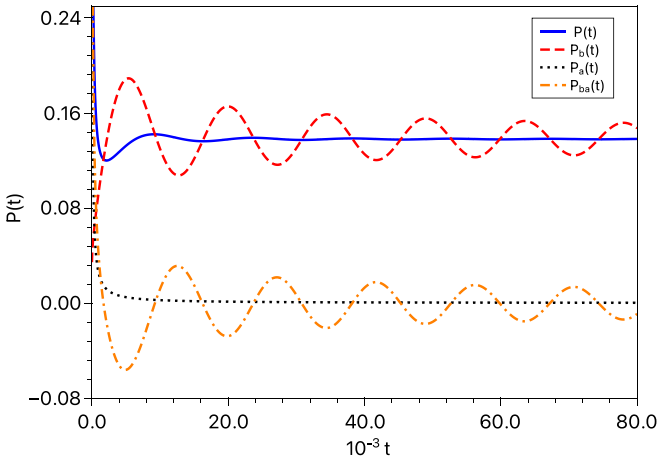

FIG. 2. Plot of the nonescape probability $P(t)$ vs the time t in natural units according to Eq. (29) as indicated in the legend. It is worth noticing the oscillatory behavior of the bound-state contribution $P_b(t)$, which is almost canceled by that arising from the interference term $P_{ba}(t)$. See text.

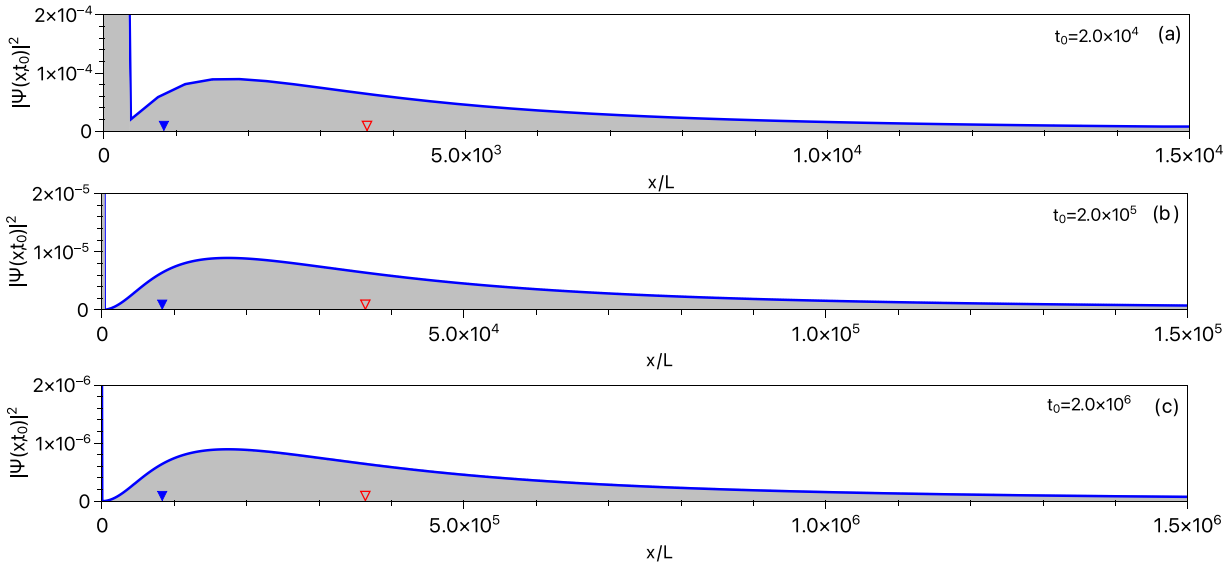

FIG. 3. Probability density $|\Psi(x_0,t)|^2$ as a function of distance along the external interaction region in units of the potential width x/L. The panels refer to distinct distance spans and fixed times to show that the bump structure propagates through space. The blue solid and red open triangles follow from the distances $x_b = 2\gamma_b t_0$ and $x_a = 2\gamma_a t_0$, respectively. See text.

Figure 4 displays the probability density and its distinct components, as given by Eqs. (35)–(38), as a function of distance x/L with the aim of determining how the "bump" shown in Fig. 3 originates. The distinct contributions are specified in the legend. We see that although the bump structure arises from the combined contribution of the bound, antibound, and interference contributions, the interference contribution plays the relevant role in the formation of the bump structure.

In the calculations discussed above, the bound-state contribution is $|C_b|^2 = 0.3693$, which implies, in view of (41), that the contribution of the continuum accounts for almost 2/3 of the weight. As a consequence, we see that the calculation of the probability density along the external interaction region as a function of time might be a cumbersome numerical task in the case of the standard Hermitian approach.

VIII. CONCLUDING REMARKS

We have shown, by considering an analytical exact non-Hermitian formulation of quantum tunneling decay entailing the antibound and resonant states of a system, that an appropriate choice of the initial state may favor a decay process involving a bound state and an antibound state close to the energy threshold. This implies a decaying process in which the contribution of the resonant states of the problem is negligible. As a consequence, the square of the expansion coefficients of the bound and antibound states adds almost to unity, and the corresponding probability density exhibits a non-negligible interference contribution that originates a bump structure that spreads in space. This bump structure does not exhibit a sharp wave front, like what occurs for proper resonant states [11],

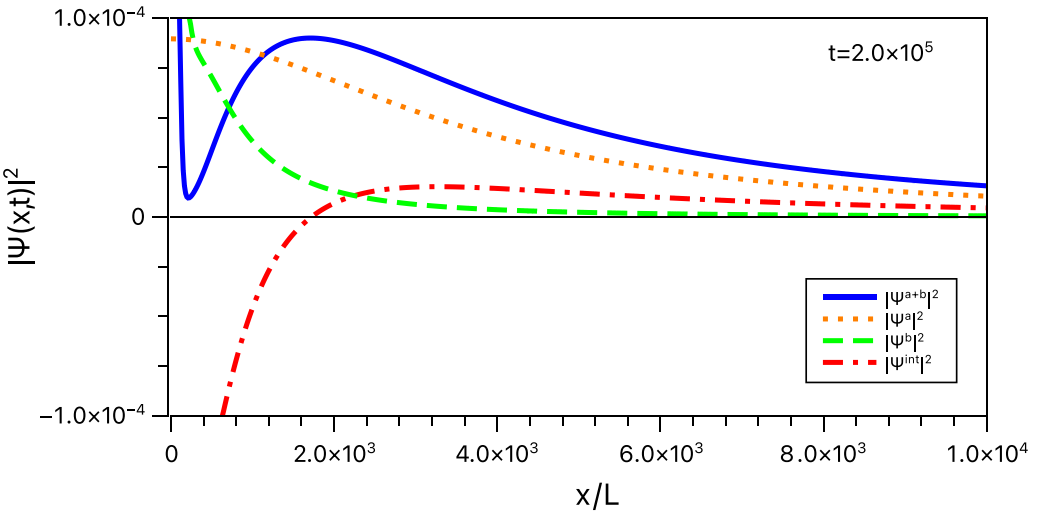

FIG. 4. Probability density $|\Psi(x_0,t)|^2$ as a function of distance along the external interaction region in units of the potential width x/L at the time $t_0 = 20\,000$, as indicated in Fig. 3(a), but with a shorter span of the distance (blue solid line). Shown are the contributions of the antibound pole (orange dotted line), bound pole (green dashed line), and the corresponding interference (red dash-dotted line) following Eqs. (35)–(38), which allow us to see how the transient bump originates. See text.

but evolves in a purely nonexponential fashion. We believe that this constitutes a decaying regime that might be accessible to experiment in artificial quantum systems. It is of interest to stress the relevant role played by the initial decaying states, which generally has been overlooked and suggests the need to investigate novel ways to generate them in a controlled form. The interference shown between bound and antibound states suggests some sort of underlying correlation involving these states that cannot be ascribed to time-reversal invariance like for resonant states and may deserve further study.

APPENDIX A: ANALYSIS OF THE BOUND AND ANTIBOUND CONTRIBUTIONS TO THE NONESCAPE PROBABILITY

One may learn about the behavior with time of $P_b(t)$, $P_a(t)$, and $P_{ba}(t)$, given by Eqs. (31), and (32) in Sec. IV, by inspecting the arguments of the transient functions $M(y_b^\circ)$ and $M(y_a^\circ)$. Note from (12) that the argument of $M(y_b^\circ)$ may be written as

$$y_b^\circ = -(\hbar/2m)(1/\sqrt{2})\gamma_b t^{1/2} + i(\hbar/2m)(1/\sqrt{2})\gamma_b t^{1/2}, \quad \text{(A1)}$$

which fulfills $(\pi/2) < \arg(y_b^\circ) < (3\pi/2)$ and therefore implies that [11,29]

$$M(y_b^\circ) = \exp(-iE_b t/\hbar) - M(-y_b^\circ), \quad \text{(A2)}$$

where $E_b = -(\hbar^2/2m)\gamma_b^2$. The above expression exhibits the usual oscillatory exponential behavior of a bound state plus a transient-term contribution $M(-y_b^\circ)$ whose argument satisfies $-(\pi/2) \arg(-y_b^\circ) < (\pi/2)$, which implies a nonexponential behavior that vanishes at long times as an inverse power of time [11,15]. Applying the above analysis to $M(y_a^\circ)$ yields at all times a purely nonexponential behavior for this quantity that at long times also goes as an inverse power of time.

APPENDIX B: ANALYSIS OF THE BOUND AND ANTIBOUND CONTRIBUTIONS TO THE PROBABILITY DENSITY ALONG THE EXTERNAL INTERACTION REGION

As mentioned in Sec. IV, along the external interaction region the decaying solution may be written as a linear combination of the bound and antibound contributions given by (34), which leads to the probability density given by (35), where the corresponding bound $[|\Psi_b(x,t)|^2]$, antibound $[|\Psi_a(x,t)|^2]$, and interference $[I_{ba}(x,t)]$ contributions are given by (36), (37), and (38).

One may follow an analysis of the transient functions $M(y_b)$, $M(y_a)$, and $M^*(y_a)$ appearing in these expressions in a fashion similar to that for the nonescape probability, except that along the external interaction region the argument of the transient functions depends on x, as shown by (11). For the function $M(y_b)$, it follows, using (11) for a given time t_0, that the corresponding argument may be written as

$$y_b = \frac{1}{2}\left(\frac{m}{\hbar t_0}\right)^{1/2}\left[(x-L) - \frac{\hbar\gamma_b}{m}t_0\right] - i\frac{1}{2}\left(\frac{m}{\hbar t_0}\right)^{1/2}\left[(x-L) + \frac{\hbar\gamma_b}{m}t_0\right]. \quad \text{(B1)}$$

One may note that if $(x-L) < \hbar\gamma_b t_0/m$, then $\pi/2 < \arg(y_b) < 3\pi/2$, and hence [11,29],

$$M(y_b) = \exp(-\gamma r)\exp(-iE_b t/\hbar) - M(-y_b), \quad \text{(B2)}$$

which exhibits both the exponential decaying behavior with distance of the bound state and the usual exponential oscillatory behavior with energy plus an additional term with an argument $-y_b$ that fulfills $-\pi/2 < \arg(-y_b) < \pi/2$ and hence gives, like for the nonescape probability, a purely nonexponential behavior. Similarly, it follows immediately from inspection of (B1) that for $(x-L) > \hbar\gamma_b t_0/m$ the corresponding argument also fulfills $-\pi/2 < \arg(y_b) < \pi/2$, and hence, $M(y_b)$ exhibits a purely nonexponential behavior at all times. Following a similar procedure for $M(y_a)$ in (37), one may write the corresponding argument as

$$y_a = \frac{1}{2}\left(\frac{m}{\hbar t_0}\right)^{1/2}\left[(x-L) + \frac{\hbar\gamma_a}{m}t_0\right] - i\frac{1}{2}\left(\frac{m}{\hbar t_0}\right)^{1/2}\left[(x-L) - \frac{\hbar\gamma_a}{m}t_0\right], \quad \text{(B3)}$$

which satisfies $-\pi/2 < \arg(y_b) < \pi/2$, which implies that $M(y_a)$ behaves in a purely nonexponential fashion at all times. It is easily seen that a similar situation occurs for $M^*(y_a)$.

[1] G. Gamow, Z. Phys. **51**, 204 (1928).
[2] G. Gamow, Nature (London) **122**, 805 (1928).
[3] L. A. Khalfin, Sov. Phys. JETP **6**, 1053 (1958).
[4] L. A. Khalfin, JETP Lett. **8**, 65 (1968).
[5] L. Fonda, G. C. Ghirardi, and A. Rimini, Rep. Prog. Phys. **41**, 587 (1978).
[6] A. Peres, Ann. Phys. (NY) **129**, 33 (1980).
[7] G. García-Calderón, Adv. Quantum Chem. **60**, 407 (2010).
[8] E. Torrontegui, J. G. Muga, J. Martorell, and D. W. L. Sprung, Adv. Quantum Chem. **60**, 485 (2010).
[9] G. García-Calderón, I. Maldonado, and J. Villavicencio, Phys. Rev. A **76**, 012103 (2007). Note the typo in Eq. (15). It should read $\mathrm{Re}\{\sum_{p=1}^{\infty} C_p \bar{C}_p\} = 1$. Another typo appears in Eq. (47), where the quantity on the right-hand side should be the absolute value squared.
[10] S. Cordero and G. García-Calderón, Phys. Rev. A **86**, 062116 (2012).
[11] G. García-Calderón and R. Romo, Ann. Phys. (NY) **424**, 168348 (2021).
[12] G. García-Calderón and R. Romo, Europhys. Lett. **139**, 60001 (2022).
[13] A. Ludviksson, J. Phys. A **20**, 4733 (1987).
[14] R. G. Newton, *Scattering Theory of Waves and Particles*, 2nd ed. (Dover, New York, 2002), Chap. 12.
[15] G. García-Calderón, A. Máttar, and J. Villavicencio, Phys. Scr. **2012**, 014076 (2012).

[16] G. García-Calderón and R. E. Peierls, Nucl. Phys. A **265**, 443 (1976).
[17] G. García-Calderón and A. Rubio, Phys. Rev. A **55**, 3361 (1997).
[18] H. Nussenzveig, Nucl. Phys. **11**, 499 (1959).
[19] E. Süli and D. F. Mayers, *An Introduction to Numerical Analysis* (Cambridge University Press, Cambridge, 2003).
[20] V. N. Faddeyeva and M. N. Terentev, *Tables of Values of the Function* $\omega(z) = e^{-z^2}(1 + \frac{2i}{\sqrt{\pi}} \int_0^z e^{t^2} dt)$*, for Complex Argument*, edited by V. A. Fock (Pergamon, London, 1961).
[21] M. Abramowitz and I. Stegun, *Handbook of Mathematical Functions* (Dover, New York, 1968), Chap. 7.
[22] G. P. M. Poppe and C. M. J. Wijers, ACM Trans. Math. Software **16**, 38 (1990).
[23] G. García-Calderón and R. Romo, Phys. Rev. A **93**, 022118 (2016).
[24] M. Tsuchiya, T. Matsusue, and H. Sakaki, Phys. Rev. Lett. **59**, 2356 (1987).
[25] G. García-Calderón and J. Villavicencio, Phys. Rev. A **73**, 062115 (2006).
[26] F. Serwane, G. Zürn, T. Lompe, T. Ottenstein, A. N. Wenz, and S. Jochim, Science **332**, 336 (2011).
[27] J. Humblet and L. Rosenfeld, Nucl. Phys. **26**, 529 (1961).
[28] G. García-Calderón and A. Rubio, Nucl. Phys. A **458**, 560 (1986).
[29] M. Moshinsky, Phys. Rev. **88**, 625 (1952).